

Running title: Quantification of Prx inactivation

Evaluating peroxiredoxin sensitivity towards inactivation by peroxide substrates

Kimberly J. Nelson¹, Derek Parsonage¹, P. Andrew Karplus^{*2}, and Leslie B. Poole^{*1}

¹Department of Biochemistry, Wake Forest School of Medicine,
Winston-Salem, NC 27157

²Department of Biochemistry and Biophysics, Oregon State University
Corvallis, Oregon 97333

*Corresponding authors: lbpoole@wakehealth.edu, Tel: 336-716-6711, Fax: 336-713-1283;
karplusp@science.oregonstate.edu, Tel: 541-737-3200, Fax: 541-737-0481

Keywords (5-10): peroxidase, redox signaling, peroxide signaling, oxidative inactivation, cysteine sulfinic acid, cysteine sulfenic acid, hyperoxidation, mass spectrometry

Contents

1. Introduction
 - 1.1 Background
 - 1.2 Theory of the peroxide dependence of sensitivity
2. Materials
 - 2.1 Solutions
 - 2.2 Proteins
3. Measuring inactivation sensitivity by steady-state NADPH-linked assays
 - 3.1 Evaluation of peroxide sensitivity of *E. coli* thiol peroxidase (Tpx) with thioredoxin (Trx1) and thioredoxin reductase (TrxR)
 - 3.1.1 *Demonstration of linear relationship between reaction rate and Prx concentration and establishment of the range of peroxide concentrations where inactivation is observed*
 - 3.1.2 *Data fitting and analysis*
 - 3.2 Evaluation of substrate specificity for inactivation
 - 3.2.1 *Tpx inactivation by CHP vs. H₂O₂*
 - 3.2.2 *Tpx inactivation by CHP in the presence of different reductants (E. coli Trx1 vs. Trx2)*
 - 3.2.3 *Inactivation of S. typhimurium AhpC by different hydroperoxide substrates*
4. Measuring inactivation sensitivity by multi-turnover cycling with ROOH and DTT followed by mass spectrometry analysis
5. Measuring inactivation sensitivity of Prx1/AhpC peroxiredoxins under single turnover conditions followed by gel electrophoresis
6. Conclusions/Summary

Abstract

Peroxiredoxins (Prxs) are very effective peroxide reducing enzymes, but also are susceptible to being oxidatively inactivated by their own substrates. The level of sensitivity to such hyperoxidation varies depending both on the enzyme involved and the type of peroxide substrate. For some Prxs, the hyperoxidation has physiological relevance, so it is important to define approaches that can be used to quantify sensitivity. Here we describe three distinct approaches that can be used to obtain quantitative or semiquantitative estimates of Prx sensitivity and define $C_{\text{hyp}1\%}$ as a simple way of quantifying sensitivity so that values can easily be compared.

1. Introduction

1.1 Background

Peroxiredoxins (Prxs) are a widespread family of cysteine-dependent peroxidases that appear to be the dominant peroxidases in many organisms [reviewed in (Hall *et al.*, 2009; Winterbourn, 2008)]. The Prx catalytic cycle centers around an active site cysteine (Cys) residue (C_p for peroxidatic Cys) that is oxidized to Cys-sulfenic acid (C_p -SOH), then reacts with another (resolving) thiol to make a disulfide, that is in turn reduced to regenerate the substrate-ready form of the enzyme (Figure 1). An additional key point is that in this enzyme family, the C_p residue in the fully-folded active site is protected and a local unfolding event must occur prior to disulfide formation. It is now well established that certain Prxs are readily inactivated by hydrogen peroxide at submillimolar concentrations (Chae *et al.*, 1994; Yang *et al.*, 2002), whereas others are much less sensitive (Wood *et al.*, 2003). This oxidative inactivation, or 'hyperoxidation', occurs when a second molecule of peroxide reacts with the C_p -SOH to make Cys-sulfinic acid (or sulfinate, C_p -SO₂⁻), which also can even be further oxidized by a third peroxide to Cys-sulfonic acid (or sulfonate, C_p -SO₃⁻) (Figure 1).

Introducing the terms "sensitive" and "robust" to characterize the two peroxiredoxins compared in their study, Wood *et al.* (2003) showed that the sensitivity to oxidative inactivation is caused by structural features that slow disulfide formation (step 3 of Figure 1), lengthening the lifetime of the C_p -SOH intermediate, thereby allowing it more time to react with a second peroxide (Wood *et al.*, 2003). It was further proposed that the sensitivity of certain eukaryotic Prxs has been selected for during evolution because it allows these enzymes to remove hydrogen peroxide under normal conditions, but (by being inactivated) allows hydrogen peroxide to locally build up and oxidize specific target proteins when the peroxide is purposefully produced as a part of a signaling pathway. Such a 'floodgate' type

of behavior has recently been shown to occur for the mitochondrial enzyme Prx3 in the regulation of cortisone production (Kil *et al.*, 2012). Although much still remains to be learned about the physiological role(s) of Prx hyperoxidation, the existence of sulfiredoxin, an ATP-dependent reactivator of hyperoxidized Prx (Biteau *et al.*, 2003; Lowther and Haynes, 2011) that is inducible (Jeong *et al.*, 2012) and important for the survival of cells under low (10-20 μ M) peroxide exposure (Baek *et al.*, 2012), underscores the physiological relevance of Prx hyperoxidation.

By using antibodies specific for sulfinic and sulfonic acid, numerous examples have been found of Prx hyperoxidation in biologically relevant systems. Recently, in one such study, Prx hyperoxidation was seen to occur as part of what was proposed to be an ancient circadian rhythm that occurs in very diverse organisms (Edgar *et al.*, 2012). Given the need to better understand the physiological roles of Prx hyperoxidation, it is important to be able to characterize this property for any given Prx. Furthermore, since sensitivity to hyperoxidation is a continuous rather than a binary property, it is an oversimplification to characterize enzymes as simply “sensitive” or “robust”; instead, what is needed is a set of approaches to quantify and compare the level of sensitivity of Prxs. Studies using Western blots specific for hyperoxidized Cys residues are of limited use both because they provide qualitative rather than quantitative data, and because the antibodies available typically recognize sulfonic acid more strongly than sulfinic acid. Mass spectrometry and isoelectric focusing are in principle useful, but have not yet been applied to provide information about the relative sensitivity to hyperoxidation of various proteins or variants. Here, we describe three methods for making such quantitative or semi-quantitative comparisons. We apply these methods variously to demonstrate the high degree of insensitivity of bacterial AhpC toward H_2O_2 inactivation, to quantify the relative sensitivities of *E. coli* Tpx toward inactivation by cumene hydroperoxide versus hydrogen peroxide, and also to explore the previously uncharacterized sensitivity of Cp20, an unusual glutaredoxin (Cp9) dependent Prx from *Clostridium pasteurianum*.

1.2 Theory of the peroxide dependence of sensitivity

In our earlier work (Wood *et al.*, 2003), we briefly presented a model for how the rate of inactivation observed would be expected to vary with the concentration of peroxide used in the assay, and we explain this more fully here. When any Prx reacts with a peroxide, the sulfenic acid formed at the active site can then either form a disulfide bond with a resolving SH group (Figure 1, steps 2a and 3), or react with a second peroxide to undergo irreversible inactivation (Figure 1, step 2b). The partitioning of the sulfenic acid into the two pathways during turnover depends on several rates associated with chemistry and conformational changes, because disulfide bond formation requires a conformational change from fully folded (FF) to locally unfolded (LU), and the hyperoxidation reaction occurs in the fully-folded enzyme. The estimated rates of conformational change are quite large for one Prx (Perkins *et al.*, 2012), suggesting that this can be treated as a rapid equilibration step with the equilibrium constant for locally-unfolded relative to fully-folded enzyme defined as K_{LU} . Defining rate constants for disulfide bond formation and hyperoxidation as k_{SS} and k_{SO_2H} , respectively (Figure 1), the rate of disulfide bond formation is $k_{SS}[E_{LU}]$ (where $[E_{LU}]$ is the concentration of locally-unfolded enzyme) and the rate of inactivation is $k_{SO_2H}[ROOH][E_{FF}]$. Neither reaction is chemically reversible (back to the sulfenic acid) under physiological conditions. Combining these, the fraction of protein that is inactivated during each catalytic cycle can be described by

$$f_{inact} = \frac{k_{SO_2H}[ROOH][E_{FF}]}{k_{SO_2H}[ROOH][E_{FF}] + k_{SS}[E_{LU}]}$$

Dividing the numerator and denominator by $[E_{FF}]$, and, assuming that the FF and LU forms are in rapid equilibrium so that the ratio $[E_{LU}]/[E_{FF}]$ can be replaced by K_{LU} , we get

$$f_{inact} = \frac{k_{SO_2H}[ROOH]}{k_{SO_2H}[ROOH] + k_{SS}K_{LU}}$$

Then, as was described in our earlier paper (Wood *et al.*, 2003), when f_{inact} is <0.1 , the first term in the denominator is small compared with the second one, and so the above relationship can be approximated as

$$f_{inact} \approx \frac{k_{SO_2H}[CHP]}{k_{SS}K_{LU}}$$

Thus, f_{inact} under these limiting conditions is expected to be linearly dependent on peroxide concentration. This also makes clear that for given values of k_{SO_2H} and k_{SS} , the stabilization of the FF conformation of Prxs (i.e., a lowering of K_{LU}) will have the effect of increasing f_{inact} , making the enzyme more sensitive. That f_{inact} only depends on the parameters noted means that it should not depend on the identity of the reductant used for the recycling of the disulfide form back to the dithiol form. With this in mind, one can potentially carry out the kinds of studies described here using reductants ranging from something as general as dithiothreitol (DTT) to something as specific as the true physiological partner protein. Also, we note that by reporting the sensitivity in terms of the fraction of molecules inactivated per catalytic cycle, given a constant amount of peroxide substrate, the total level of inactivation will depend directly on how many catalytic cycles have occurred.

As can be seen, the value of f_{inact} itself for a given peroxide is not an intrinsic property of the enzyme, but depends on the peroxide concentration used. Previously (Wood *et al.*, 2003), to establish a value that depends just on the enzyme and the type of peroxide, we reported the sensitivity as the slope of the $f_{inact}/[H_2O_2]$ line, which approximates $k_{SO_2H}/(k_{SS}K_{LU})$; for human PrxI reactivity toward H_2O_2 , the value was 162 M^{-1} . This value implies that given a 6.2 mM solution of H_2O_2 (the reciprocal of the slope), all Prx molecules will inactivate in a single catalytic cycle (i.e., $f_{inact}=1$). Unfortunately, this

manner of reporting the sensitivity is not especially meaningful, in part because the equation used to derive it is an approximation only valid up to an f_{inact} value of 0.1. For this reason, we here suggest that a more intuitively and physiologically meaningful way to report the sensitivity would be to report the concentration of peroxide at which f_{inact} would have a value of 0.01 (i.e. 1%). This corresponds to the peroxide concentration at which 1 out of every 100 Prx molecules would be inactivated per turnover and can be calculated as the inverse of the above-mentioned slope divided by 100. For human PrxI, this works out to 6.2×10^{-5} M, or 62 μM H_2O_2 . Here, we will call this quantity $C_{hyp1\%}$, as in $C_{hyp1\%}=62 \mu\text{M}$ for human PrxI hyperoxidation by H_2O_2 . At this concentration the half-life for activity is about 70 turnovers, which given the k_{cat} for these enzymes near 60 s^{-1} , could be as fast as $\sim 1.2 \text{ s}$ under conditions where the catalytic reaction with H_2O_2 is the rate-limiting step.

2. Materials

2.1 Solutions

25 mM potassium phosphate, pH 7.0, 1 mM EDTA, with 100 mM ammonium sulfate (assay buffer)

25 mM potassium phosphate, pH 7.0, 1 mM EDTA (standard buffer)

15 mM NADPH, dissolved in 10 mM Tris- SO_4 , pH 8.5

100 mM cumene hydroperoxide (CHP), dissolved first in dimethyl sulfoxide (DMSO) to make a 100 mM stock; standardized (Nelson and Parsonage, 2011)

100 mM hydrogen peroxide, standardized (Nelson and Parsonage, 2011; Poole and Ellis, 2002)

100 mM dithiothreitol (DTT)

5x non-reducing sample buffer with 100 mM N-ethylmaleimide, 250 mM Tris/HCl pH 6.8, 50 % (vol/vol) glycerol, 10 % sodium dodecyl sulfate, 0.2 % bromophenol blue

2.2 Proteins

All proteins used were recombinantly expressed and purified as described previously:

E. coli Trx1 and Trx2 (Reeves *et al.*, 2011)

E. coli TrxR (Poole *et al.*, 2000)

E. coli Tpx (Baker and Poole, 2003)

S. typhimurium AhpC (Poole and Ellis, 1996)

Clostridium pasteurianum Cp20 (Reynolds *et al.*, 2002)

3. Measuring inactivation sensitivity by steady-state NADPH-linked assays

3.1 Evaluation of peroxide sensitivity of *E. coli* thiol peroxidase (Tpx) with thioredoxin (Trx1) and thioredoxin reductase (TrxR)

3.1.1 *Demonstration of linear relationship between reaction rate and Prx concentration and establishment of the range of peroxide concentrations where inactivation is observed*

As has been shown previously, the inactivation of sensitive Prx proteins can be identified by observation of the kinetic traces during turnover in the presence of μM to mM concentrations of peroxide substrates and a suitable reductant (Baker and Poole, 2003; Wood *et al.*, 2003; Yang *et al.*,

2002). As the Prx protein becomes hyperoxidized over the course of the reaction (with a fraction inactivated during each turnover), the kinetic trace increasingly deviates from the linear kinetics expected for the portion of the reaction having peroxide concentrations significantly above the apparent K_M . The example Prx analyzed in detail here is the Tpx protein from *E. coli*, which was reported to be sensitive to inactivation during turnover with cumene hydroperoxide (CHP) and 15-hydroperoxyeicosatetraenoic acid, but not hydrogen peroxide (Baker and Poole, 2003). The previous enzymological analysis of Tpx established the kinetic parameters for catalytic turnover using thioredoxin (Trx1), thioredoxin reductase (TrxR), and NADPH. By varying peroxide and Trx1 concentrations in a full bisubstrate analysis, K_M values for CHP and H_2O_2 were found to be $9.1 \pm 1.8 \mu M$ and $1730 \pm 360 \mu M$, respectively, while the k_{cat} values with these two substrates were about the same, at $\sim 73 s^{-1}$. The K_M value for Trx1 was $\sim 24 \mu M$ and did not vary with different peroxides. While the inactivation during turnover of Tpx with CHP was noted to occur at concentrations of $100 \mu M$ and higher under the assay conditions used, the kinetics of inactivation was not further assessed.

In the present work, assays were designed to monitor the absorbance of the NADPH in the system containing TrxR, Trx1, Tpx and CHP over multiple turnovers. Briefly, a “master mix” of TrxR, Trx, and Tpx was made in standard assay buffer and then divided into multiple cuvettes ($270 \mu L$ each). NADPH was added ($20 \mu L$) and the solution was mixed, and then a 30X peroxide solution ($10 \mu L$) was added and mixed as quickly as possible to start the assay. The 30X stock CHP solutions all contained an equal amount of DMSO (final concentration in the assays was 0.14%). For all peroxide concentrations, the rate of NADPH oxidation in the absence of Prx was measured and TrxR concentrations were kept very low ($0.05 \mu M$) in these assays to minimize the Tpx-independent loss of NADPH over these extended incubation periods. From the data shown in Fig. 2a using $50 \mu M$ CHP, an average of 500 turnovers for Tpx in each of the enzymes samples was complete by ~ 5 min; assays were typically monitored over 15 to 20 min.

For experiments like this one monitoring the Prx reaction rate indirectly through absorbance changes related to NADPH oxidation, it is important to establish at the outset of the studies that the rate is directly dependent on the concentration of the active Prx rather than being limited by some other component of the system. This was established in Fig. 2a by evaluating the initial rates at the very beginning of each reaction (the first ~4 points, collected in <0.5 min), which were indeed shown to be directly dependent on Tpx concentrations from 0.025 to 0.2 μM . The abrupt transition from turnover to background TrxR oxidase rates just before 6 min in Fig. 2a is due to depletion of substrate, and confirms that under these conditions, the $K_{M,app}$ for CHP is quite low, as we do not observe a significant change in rate until the CHP is almost completely depleted.

Given our results from Fig. 2a, we chose to study turnover and inactivation of Tpx with CHP using 0.1 μM Tpx and 50 to 150 μM CHP. As emphasized in Fig. 2b, the initial rate of turnover with Tpx is the same at all concentrations (reflecting the amount of active Tpx), but the divergence from linearity due to inactivation occurs to a greater extent at the higher CHP concentrations where the rate of inactivation is expected to increase.

3.1.2 Data fitting and analysis

In order to analyze the data obtained with Tpx to determine f_{inact} , we began with an analysis of the “instantaneous” rates of reaction over a short slice of time (from slopes across 5 time points) using a linear fit and a moving window (sliding by one point each time) of the data in an Excel spreadsheet. Rates of NADPH oxidation were first corrected for the background rate in the absence of Tpx and then converted to μM NADPH oxidized per min by dividing the $\Delta A_{340}/\text{min}$ value by the molar extinction coefficient for NADPH, $6200 \text{ M}^{-1} \text{ cm}^{-1}$. Using a logarithmic scale for the *rate* axis demonstrates that the data obey pseudo-first order decay kinetics as expected given that CHP is in significant excess and changing very little during the assay (Fig. 3). The slopes of these lines yield k_{inact} (equal to k_{SO_2H}

[CHP]), which can then be divided by the initial (turnover) rate in order to obtain f_{inact} at each CHP concentration.

For this work, we were also able to develop and validate a complementary approach whereby the exponential decay rate is determined using a direct fit to an equation including both linear and exponential decay terms (fits by this approach are shown in Fig. 2).

$$y = a \cdot e^{-kt} + b \cdot t + c$$

where y is absorbance at time t , k is the exponential rate of decay in activity, and a , b and c are coefficients that are floated during the fit. We found, in practice, that a reliable value for k can only be obtained where there is sufficient curvature in the line so that a simple linear fit of the data gives $R < 0.995$. We also determined through many repetitions that the fit to yield k was of high quality only if the error on this fit value was $< 2-3\%$. Either raw absorbance data or data converted to units of rates can be used for these fits, and background rates of absorbance changes in the absence of Tpx do not have to be subtracted prior to fitting the data as long as the background loss in absorbance over time is linear (as observed in our data, Fig. 2a, no Tpx).

Using multiple determinations and the NADPH-TrxR-Trx1-Tpx system, the slope of the $f_{inact}/[\text{CHP}]$ line, which approximates $k_{\text{SO}_2\text{H}}/(k_{\text{SS}} K_{\text{LU}})$, is 64 M^{-1} (Fig. 4). Given this value, $C_{\text{hyp}1\%} = 156 \text{ }\mu\text{M}$ for *E. coli* Tpx with CHP. Comparing this to the $C_{\text{hyp}1\%}$ of $62 \text{ }\mu\text{M}$ with H_2O_2 for human Prx I, one can see that Tpx is not quite as sensitive toward CHP as human Prx I is toward H_2O_2 .

3.2 Evaluation of substrate specificity for inactivation

3.2.1 Tpx inactivation by CHP vs. H_2O_2

In the original kinetic analysis of Tpx, K_M values for CHP and H_2O_2 were shown to be very different (9.1 and 1730 μM , respectively), and only the CHP was reported to cause inactivation during turnover (Baker and Poole, 2003). In order to further explore the differences between these two substrates under conditions more suitable to measuring inactivation, we conducted the assays of Tpx with H_2O_2 over the same concentrations as CHP. Even though initial rates were somewhat different with the two peroxides at 100 and 250 μM (reflecting the higher K_M for H_2O_2), the H_2O_2 traces are quite linear making it clear that, unlike CHP, H_2O_2 does not significantly inactivate Tpx during turnover under these conditions (Fig. 5). The inactivating effect of H_2O_2 was difficult to detect below mM levels, and above 1 mM H_2O_2 , the background (Tpx-independent) NADPH oxidation becomes high and obfuscates the analysis. With a single determination at 1 mM H_2O_2 , an approximate value of $0.5 M^{-1}$ was obtained for $f_{inact}/[H_2O_2]$, corresponding to $C_{hyp1\%} \sim 20,000 \mu M$ indicating (by comparison with the $C_{hyp1\%} = 156 \mu M$ for CHP) that there is a >100-fold difference in sensitivity of Tpx for inactivation by these two hydroperoxides. Further evaluation of these two substrates as inactivators of Tpx was also conducted using complementary methods, as described in section 4.

3.2.2 Tpx inactivation by CHP in the presence of different reductants (*E. coli* Trx1 vs. Trx2)

As the analysis of f_{inact} involves the determination of the pseudo-first order rate of decay in activity adjusted for turnover rates, we hypothesized that a sensitive Prx would exhibit its characteristic peroxide sensitivity with even a relatively poor reductant as long as a sufficient number of turnovers are measured. In order to test this hypothesis, we conducted the assays described above with Tpx and CHP swapping in *E. coli* Trx2 in place of Trx1. In earlier studies of Tpx, Trx1 was shown to be a much better substrate than Trx2 (Baker and Poole, 2003). We evaluated the activity of Tpx with Trx2 using assay conditions similar to those above (0.3-0.6 μM Tpx, 100 μM NADPH, 0.05 μM TrxR, and 50 μM CHP) and found that the rate of turnover with Tpx and 10 μM Trx2 was 5.4-fold slower than with Tpx and 10 μM Trx1.

Upon evaluation of the inactivation and turnover rates of Tpx with Trx2 (using 2 μM Trx2 rather than 1 μM to partially compensate for the difference in rates between the two), the $C_{\text{hyp}1\%}$ was 217 μM for CHP (Fig. 4). Thus, the inactivation profiles observed for Tpx with CHP with either the more efficient reductant, Trx1, or the poorer reductant, Trx2, differ by less than a factor of 1.4.

To also ask whether the generic chemical reductant dithiothreitol (DTT) could be used in similar assays, we conducted a set of studies to evaluate inactivation with this relatively slow reductant of Tpx. Unfortunately, there is no strong spectral feature that changes between reduced and oxidized DTT that could be used to monitor reaction rates, so an endpoint assay utilizing ferrous ammonium sulfate and Xylenol Orange (a FOX assay) was conducted to monitor peroxide levels over time (Nelson and Parsonage, 2011). Due to the low rate of reaction between Tpx and DTT, a high concentration of Tpx (5 μM) was required to observe significant changes in peroxide concentration. Because of the noise in the experimental data, which is relatively large, and the small fraction of Tpx inactivated with so few turnovers, we were unable to use this assay to measure any significant inactivation of Tpx with CHP.

3.2.3 Inactivation of *S. typhimurium* AhpC by different hydroperoxide substrates

It was clear in our previous work with *S. typhimurium* AhpC, a rather robust Prx (Wood *et al.*, 2003), that the quality of the inactivation data used to assess AhpC sensitivity by this method was marginal due to the 10-30 mM levels of H_2O_2 required to collect these data; at these peroxide concentrations, Prx-independent background rates of NADPH oxidation are significant. In later work by our group, the acquisition time was increased to better observe the curvature associated with inactivation and to allow comparisons of the relatively robust AhpC with even less sensitive proteins (Parsonage *et al.*, 2010; Parsonage *et al.*, 2005). Reexamining our previously published data investigating the

sensitivity of *S. typhimurium* AhpC toward different peroxide substrates (Parsonage *et al.*, 2008), we were able to fit data at 10 and 30 mM ethyl hydroperoxide using our new direct fit to the combined linear and exponential decay model, although only the 30 mM data yielded a rate of inactivation that matched our criteria above for extracting reliable rates as described in Section 3.1.2. Using this value and the initial rate of the reaction, and assuming a linear relationship through the origin, the $f_{\text{inact}}/[\text{ethyl hydroperoxide}]$ value was calculated to be 0.98 M^{-1} . We note that this is quite similar to our previously reported value for H_2O_2 of $1.4 \pm 0.3 \text{ M}^{-1}$ (Wood *et al.*, 2003). Thus, $C_{\text{hyp}1\%}$ is $\sim 10,000 \text{ }\mu\text{M}$ for both ethyl hydroperoxide or H_2O_2 with *S. typhimurium* AhpC. Exploring inactivation with bulky hydroperoxides like CHP and t-butyl hydroperoxide, which exhibited higher K_M values with AhpC than did ethyl hydroperoxide and H_2O_2 , we found that these substrates were not prone to hyperoxidize AhpC during turnover to any detectable degree based on a qualitative evaluation of the data (Parsonage *et al.*, 2008). Thus, like with Tpx, peroxide substrates of AhpC exhibiting high K_M values do not significantly promote inactivation during turnover.

4. Measuring inactivation sensitivity by multiturnover cycling with ROOH and DTT followed by mass spectrometry analysis

As described above, monitoring inactivation by the decrease in activity during continuously-monitored assays has many advantages, including quantitative evaluation of $C_{\text{hyp}1\%}$ as a measure of inactivation sensitivity. When this value is very high, however, its accurate determination becomes more difficult as shown above. However, even very robust Prxs subjected to many turnovers in the presence of high DTT and peroxide levels can eventually be inactivated through hyperoxidation, as observed by mass spectrometry. Thus, we evaluated inactivation based on levels of $-\text{SO}_2\text{H}$ and $-\text{SO}_3\text{H}$ as assessed by mass spectrometry (MS) after addition of varying ratios of peroxide to Prx protein in order to further evaluate peroxide sensitivity of sensitive and robust enzymes. This assay is particularly convenient in having very few components (just the enzyme, the peroxide of interest and

an excess of DTT) and an incubation time that is long enough to allow for full reaction of the peroxide (overnight incubations seemed to be sufficient for this in the cases studied). Thus, it can be used even when the identity of the physiological reductant is unknown. Further, we were able to simply exchange the protein (after incubation with DTT and peroxide) into a MS-friendly buffer, 10 mM ammonium bicarbonate, before addition of acetonitrile and formic acid for MS analysis without first blocking free thiol groups by alkylation (avoiding additional sample manipulations and potential for incomplete reactions), although this requires that buffers be completely free of peroxides or metals which can promote oxidation in air. It should be noted that the degree of Prx hyperoxidation is dependent on both the number of turnovers and the peroxide concentration; in the assays conducted herein, we held the starting peroxide concentration constant (at 1 mM) and modified the number of potential turnovers by varying the Prx concentration (Fig. 6). Also, given that the peroxide is the limiting reagent and the incubation is extended to allow for all of it to react, the peroxide concentration is changing throughout the incubation, and we did not pursue a rigorous mathematical treatment of the data as described above.

Consistent with the results presented above, this approach demonstrates that Tpx is much more sensitive toward CHP than toward H_2O_2 , with half the molecules of Tpx becoming hyperoxidized in assays where the Tpx concentration is only 50 to 100-fold less than the CHP concentration (Fig. 6). AhpC hyperoxidation, like that of Tpx with H_2O_2 , is not significant even at a ratio of 2000:1 for peroxide to protein using either CHP or H_2O_2 (Fig. 6b).

5. Measuring inactivation sensitivity of Prx1/AhpC

peroxiredoxins under single turnover conditions followed by gel electrophoresis

A distinct way to assess sensitivity toward inactivation by peroxides was also developed where the reduced Prx is subjected to very high peroxide concentrations in the absence of reductant, allowing only one opportunity during this partial turnover experiment for each active site to partition between either the disulfide-bonded form or the hyperoxidized (sulfinic or sulfonic acid) forms (following steps 2a or 2b, respectively, in Fig. 1). This analysis is particularly straightforward with *S. typhimurium* AhpC, where a simple gel separation (after alkylation of free thiol groups with NEM during denaturation to prepare samples) distinguishes readily between proteins with zero, one and two disulfide bonds per dimer (Fig. 7). Because this readout reflects the competition between hyperoxidation and disulfide bond formation, and AhpC is quite significantly resistant to hyperoxidation, partitioning isn't readily observed until nearly molar levels of H₂O₂ (Fig. 7b).

Using this approach to investigate other Prxs in the Prx1/AhpC group (also known as typical 2-Cys Prxs), we found that the glutaredoxin (Cp9)-dependent Prx1/AhpC-like Cp20 protein from *Clostridium pasteurianum* (Reynolds *et al.*, 2002) was in fact highly sensitive to inactivation by H₂O₂ (Fig. 7c). This high degree of sensitivity was also observed by MS analysis after treatment with peroxide and DTT as described in the previous section. Unfortunately, the recombinantly-expressed, purified Cp20 protein is a mixture of two species due to a partial codon misread in the third position (substituting Lys for Arg in 36% of the molecules), making full detailed analysis of the various redox states by MS difficult (Reynolds *et al.*, 2002). However, it can be readily concluded that more than half of the protein is irreversibly oxidized to –SO₂H and –SO₃H upon addition of a 50-fold excess of either CHP or H₂O₂ in the presence of excess DTT, indicating that this protein is more sensitive than Tpx toward inactivation by peroxides. Assays using the *E. coli* TrxR and Trx1 system as described in Section 3 further confirmed this result and indicated that, unlike Tpx, Cp20 exhibited a similar sensitivity toward both H₂O₂ and CHP (not shown).

It should be noted that this gel approach takes significant advantage of the dimeric nature of disulfide-bonded AhpC and Cp20 given that the peroxidatic and resolving Cys residues are on different subunits. However, this method would need to be adapted to study Prxs from other groups, since outside of the Prx1/AhpC group nearly all catalytic disulfide bonds are intrasubunit disulfides and covalent dimers would not be observed. Therefore, an additional method to distinguish disulfide bonded from non-disulfide bonded species would likely be required (e.g., AMS modification to cause an observable increase in apparent molecular weight with each thiol group modified) (Åslund *et al.*, 1999).

6. Conclusions/Summary

Here we describe multiple methods that allow for the quantitation and analysis of Prx inactivation for both sensitive and robust Prx proteins. In addition to providing a simplified method of calculating f_{inact} values from steady state turnover assays in the presence of Trx, TrxR, and NADPH, we also present complementary methods to extract quantitative or semiquantitative data using MS analysis and polyacrylamide gel shift experiments. Because the fraction of Prx inactivated per turnover is dependent on the peroxide concentration, we propose that data for Prx sensitivity would be better presented as the peroxide concentration at which 1 of every 100 active sites is hyperoxidized per turnover, which we designate here as $C_{\text{hyp}1\%}$. Our analysis here provides data consistent with the expectation that the sensitivity of a given Prx to inactivation can be strongly dependent on the peroxide substrate, but does not vary significantly with different reductants.

ACKNOWLEDGMENTS

This work was supported by U. S. Public Health Service Grant GM050389 from the National Institutes of Health and by a 2011 Spark drug discovery grant from Wake Forest School of Medicine. We thank Mike Samuel for help with the mass spectrometry analyses reported in [figure 2.6](#).

REFERENCES

- Åslund, F., Zheng, M., Beckwith, J., and Storz, G. (1999). Regulation of the OxyR transcription factor by hydrogen peroxide and the cellular thiol-disulfide status. *Proc Natl Acad Sci U S A*. **96**, 6161-5.
- Baek, J. Y., Han, S. H., Sung, S. H., Lee, H. E., Kim, Y. M., Noh, Y. H., Bae, S. H., Rhee, S. G., and Chang, T. S. (2012). Sulfiredoxin protein is critical for redox balance and survival of cells exposed to low steady-state levels of H₂O₂. *J Biol Chem*. **287**, 81-9.
- Baker, L. M., and Poole, L. B. (2003). Catalytic mechanism of thiol peroxidase from *Escherichia coli*. Sulfenic acid formation and overoxidation of essential CYS61. *J Biol Chem*. **278**, 9203-11.
- Biteau, B., Labarre, J., and Toledano, M. B. (2003). ATP-dependent reduction of cysteine-sulphinic acid by *S. cerevisiae* sulphiredoxin. *Nature*. **425**, 980-4.
- Chae, H. Z., Chung, S. J., and Rhee, S. G. (1994). Thioredoxin-dependent peroxide reductase from yeast. *J Biol Chem*. **269**, 27670-8.
- Edgar, R. S., Green, E. W., Zhao, Y., van Ooijen, G., Olmedo, M., Qin, X., Xu, Y., Pan, M., Valekunja, U. K., Feeney, K. A., Maywood, E. S., Hastings, M. H., Baliga, N. S., Meroow, M., Millar, A. J., Johnson, C. H., Kyriacou, C. P., O'Neill, J. S., and Reddy, A. B. (2012). Peroxiredoxins are conserved markers of circadian rhythms. *Nature*. **485**, 459-64.
- Hall, A., Karplus, P. A., and Poole, L. B. (2009). Typical 2-Cys peroxiredoxins - structures, mechanisms and functions. *Febs J*. **276**, 2469-77.
- Jeong, W., Bae, S. H., Toledano, M. B., and Rhee, S. G. (2012). Role of sulfiredoxin as a regulator of peroxiredoxin function and regulation of its expression. *Free Radic Biol Med*.
- Kil, I. S., Lee, S. K., Ryu, K. W., Woo, H. A., Hu, M. C., Bae, S. H., and Rhee, S. G. (2012). Feedback control of adrenal steroidogenesis via H₂O₂-dependent, reversible inactivation of Peroxiredoxin III in mitochondria. *Mol Cell*. **46**, 584-94.
- Lowther, W. T., and Haynes, A. C. (2011). Reduction of cysteine sulfinic acid in eukaryotic, typical 2-Cys peroxiredoxins by sulfiredoxin. *Antioxid Redox Signal*. **15**, 99-109.
- Nelson, K. J., and Parsonage, D. (2011). Measurement of peroxiredoxin activity. *Curr Protoc Toxicol*. **Chapter 7**, Unit7 10.
- Parsonage, D., Desrosiers, D. C., Hazlett, K. R., Sun, Y., Nelson, K. J., Cox, D. L., Radolf, J. D., and Poole, L. B. (2010). Broad specificity AhpC-like peroxiredoxin and its thioredoxin reductant in the sparse antioxidant defense system of *Treponema pallidum*. *Proc Natl Acad Sci U S A*. **107**, 6240-5.
- Parsonage, D., Karplus, P. A., and Poole, L. B. (2008). Substrate specificity and redox potential of AhpC, a bacterial peroxiredoxin. *Proc Natl Acad Sci U S A*. **105**, 8209-14.
- Parsonage, D., Youngblood, D. S., Sarma, G. N., Wood, Z. A., Karplus, P. A., and Poole, L. B. (2005). Analysis of the link between enzymatic activity and oligomeric state in AhpC, a bacterial peroxiredoxin. *Biochemistry*. **44**, 10583-92.
- Perkins, A., Gretes, M. C., Nelson, K. J., Poole, L. B., and Karplus, P. A. (2012). Mapping the active site helix-to-strand conversion of CxxxxC Peroxiredoxin Q enzymes. *Biochemistry*. **51**, 7638-50.
- Poole, L. B., and Ellis, H. R. (1996). Flavin-dependent alkyl hydroperoxide reductase from *Salmonella typhimurium*. 1. Purification and enzymatic activities of overexpressed AhpF and AhpC proteins. *Biochemistry*. **35**, 56-64.
- Poole, L. B., and Ellis, H. R. (2002). Identification of cysteine sulfenic acid in AhpC of alkyl hydroperoxide reductase. *Methods Enzymol*. **348**, 122-36.
- Poole, L. B., Godzik, A., Nayeem, A., and Schmitt, J. D. (2000). AhpF can be dissected into two functional units: tandem repeats of two thioredoxin-like folds in the N-terminus mediate electron transfer from the thioredoxin reductase-like C-terminus to AhpC. *Biochemistry*. **39**, 6602-15.

- Reeves, S. A., Parsonage, D., Nelson, K. J., and Poole, L. B. (2011). Kinetic and thermodynamic features reveal that *Escherichia coli* BCP is an unusually versatile peroxiredoxin. *Biochemistry*. **50**, 8970-81.
- Reynolds, C. M., Meyer, J., and Poole, L. B. (2002). An NADH-dependent bacterial thioredoxin reductase-like protein in conjunction with a glutaredoxin homologue form a unique peroxiredoxin (AhpC) reducing system in *Clostridium pasteurianum*. *Biochemistry*. **41**, 1990-2001.
- Winterbourn, C. C. (2008). Reconciling the chemistry and biology of reactive oxygen species. *Nat Chem Biol*. **4**, 278-86.
- Wood, Z. A., Poole, L. B., and Karplus, P. A. (2003). Peroxiredoxin evolution and the regulation of hydrogen peroxide signaling. *Science*. **300**, 650-3.
- Yang, K. S., Kang, S. W., Woo, H. A., Hwang, S. C., Chae, H. Z., Kim, K., and Rhee, S. G. (2002). Inactivation of human peroxiredoxin I during catalysis as the result of the oxidation of the catalytic site cysteine to cysteine-sulfinic acid. *J Biol Chem*. **277**, 38029-36.

Figure Legends

Figure 1. The catalytic cycle and inactivation pathways of 2-Cys peroxiredoxins. The peroxidatic cysteine is depicted as the thiolate (S_p^-), sulfenic acid (S_pOH), sulfinic acid ($S_pO_2^-$) or sulfonic acid ($S_pO_3^-$), or in a disulfide with the resolving cysteine (S_r). Reaction of the thiolate with hydroperoxide substrates (step 1) in the fully folded (FF) active site results in a sulfenic acid which either flips out of the active site due to localized unfolding (LU) to generate the disulfide (steps 2a and 3), or reacts with an additional peroxide (step 2b) to become inactivated. Reductive recycling of the disulfide species (step 4) is catalyzed by a reducing system like thioredoxin and thioredoxin reductase.

Figure 2. Turnover and inactivation of *E. coli* Tpx in the presence of varying Tpx and cumene hydroperoxide (CHP) concentrations. The absorbance of NADPH was monitored at 340 nm in the presence of 150 μM NADPH, 0.05 μM *E. coli* thioredoxin reductase, 1 μM *E. coli* Trx1 and specified amounts of Tpx and CHP in standard assay buffer. Only one out of every four data points is shown. During the course of multiple turnovers, Tpx becomes increasingly inactivated and the slopes deviate from linear. Data were fit directly to a combined linear and exponential decay model as described in the text. In panel A, assays included 50 μM CHP and varying amounts of Tpx. In panel B, assays included 0.1 μM Tpx and varying CHP concentrations. Starting absorbances were intentionally staggered (by adding or subtracting a constant A_{340} to all data points in each set) in order to readily visualize the constant initial rate across CHP concentrations. Inactivation becomes more pronounced as the CHP concentration increases.

Figure 3. Changing rates of NADPH oxidation over time at various Tpx (A) or CHP (B) concentrations. First, slopes to give “instantaneous” rates were obtained by linear fitting, over a narrow window of five points at a time, of the data shown in Figure 2; the window was advanced by one point and the process repeated across the time series. Rates were calculated from the 340 nm data using the molar extinction coefficient for NADPH as described in the text. Rates were then replotted on a logarithmic scale versus time and fit to an exponential decay model. Fits did not include data beyond 90% inactivation due to the noise in the data at these levels.

Figure 4. Effect of cumene hydroperoxide concentration on fraction of inactivation per turnover of Tpx. Assays as shown in Figure 2 (including 150 μM NADPH, 0.05 μM TrxR, 0.1 μM Tpx and varying CHP concentrations) were conducted using either 1 μM Trx1 (black circles) or 2 μM Trx2 (gray squares) as the direct Tpx reductant. The fraction of inactivation per turnover (f_{inact}) was calculated by dividing the pseudo-first order rate of inactivation (determined as described in the text) by the turnover rate (the rate of NADPH oxidation divided by the Tpx concentration). Data (from 3 or more determinations at each CHP concentration) were averaged (shown with standard error bars) and fit to a line through the origin based on the equations given in the text. The slopes of the lines using Trx1 or Trx2 as reductant were 64 and 46 M^{-1} , respectively.

Figure 5. Turnover and inactivation of Tpx in the presence of either CHP or H_2O_2 . Assays were conducted with NADPH, TrxR, Trx and Tpx concentrations as in Figure 2, using hydroperoxide concentrations of 100 μM (squares) and 250 μM (circles) and either CHP (closed symbols) or H_2O_2 (open symbols). Starting absorbances were intentionally staggered (by adding or subtracting a constant A_{340} to all data points in each set) for clarity. Data with CHP were fit directly to a combined linear and exponential decay model as described in the text, whereas data with H_2O_2 were fit to a linear equation. Only one out of every four data points is shown.

Figure 6. *E. coli* Tpx is much more sensitive to hyperoxidation by CHP than by H_2O_2 , and *S. typhimurium* AhpC is insensitive to both, based on mass spectrometry (MS) after incubation with peroxide and excess dithiothreitol (DTT). Tpx or AhpC was treated overnight (in standard buffer) with 10 mM DTT and 1 mM peroxide (CHP or H_2O_2), using protein dilutions as needed in order to obtain

ratios of peroxide to protein of 50 to 2000. Samples were then exchanged into 10 mM ammonium bicarbonate using ultrafiltration (with Centricon YM-30 filtration units) for an effective dilution of the original buffer of ~100,000-fold prior to MS analysis. Shortly prior to MS analysis, samples were mixed 1:1 with acetonitrile and supplemented with 1 % formic acid, or further diluted into 50% acetonitrile with 1% formic acid as needed to obtain high quality MS data. Samples were analyzed through direct infusion and electrospray ionization using a Micromass Quattro II triple quadrupole mass spectrometer equipped with a Z-spray source. Data were processed and analyzed using MassLynx, version 3.5. Deconvoluted data shown in panel A include peaks at 17,701.6, 17,718.8, 17,737.1 and 17,051.2 representing the reduced thiol (-SH), sulfenic acid (-SOH), sulfinic acid (-SO₂H) and sulfonic acid (-SO₃H) forms, respectively (as indicated in the left panel). In each spectrum of panel A, the profile of untreated Tpx is shown as a dotted line. A summary of the data with Tpx (circles) or AhpC (squares) incubated with CHP (closed symbols) or H₂O₂ (open symbols) is shown in panel B. The approximate fraction of protein in sulfinic (-SO₂H) or sulfonic (-SO₃H) acid forms relative to all forms was calculated from the relative intensities.

Figure 7. *C. pasteurianum* Cp20 is much more sensitive to hyperoxidation by H₂O₂ than *S. typhimurium* AhpC based on partial turnover experiments and subsequent mobility in gel electrophoresis. Protein in standard assay buffer was reduced with 15-20 mM DTT for 30-60 min at room temperature. Excess DTT was removed using a PD10 desalting column (GE Healthcare). Protein was diluted to 10 μM and 25 μL aliquots were mixed with an equal volume of various concentrations of H₂O₂. After 10 min, the protein mixtures were denatured and alkylated by adding 12.5 μL of 5x non-reducing sample loading buffer containing N-ethylmaleimide (final concentrations of 20 mM NEM and 2% SDS). Samples were incubated at room temperature for a further 10 min before heating to 95 °C for 5 min to complete the denaturation. Samples of each reaction mixture (15 μL) were loaded on a 12% polyacrylamide gel, electrophoresed and stained for protein with GelCode Blue. Because of the sensitivity of Cp20 to oxidation, all buffers used in the preparation of the Cp20 samples were bubbled for at least 20 min with high purity argon, and the Cp20 solution was made anaerobic by cycles of evacuation and equilibration with argon, and exposure to air was kept to a minimum. The positions of protein markers, with sizes in kDa, are shown to the left of the gels and peroxide concentrations (in mM) are given above each lane. Oxidized or hyperoxidized species as depicted in panel A are labeled to the right in panels B and C. (B) Data for *S. typhimurium* AhpC (C) Data for *C. pasteurianum* Cp20.

Fig. 1

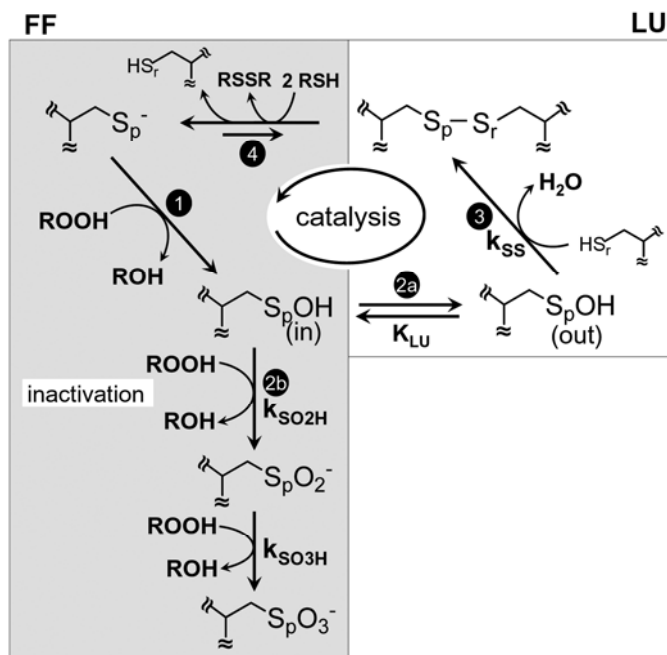


Fig. 2

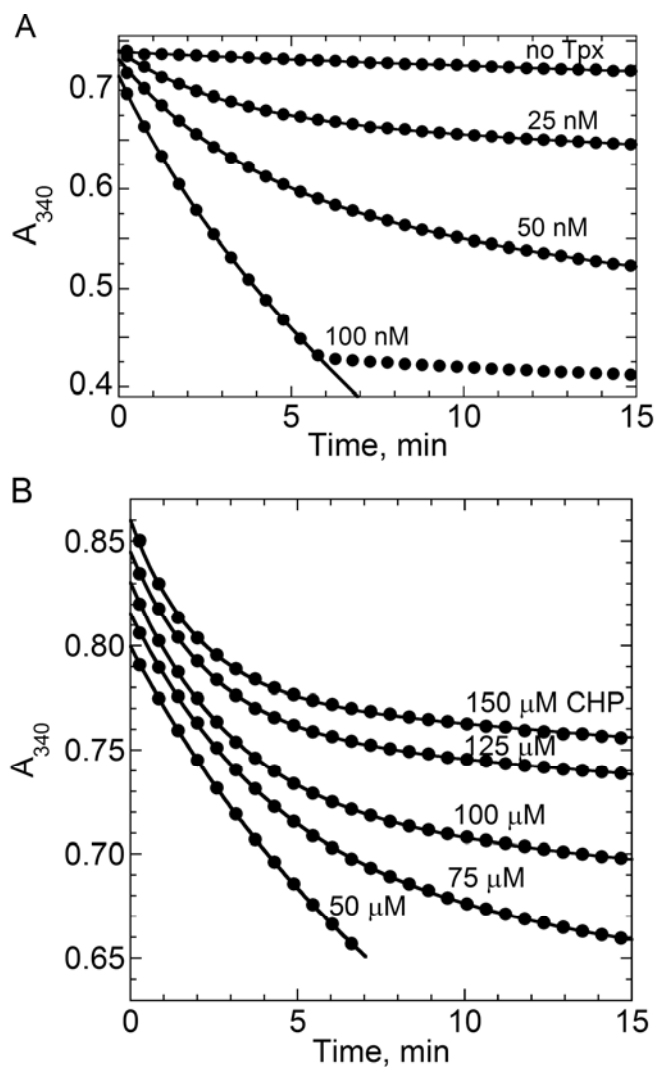


Fig. 3

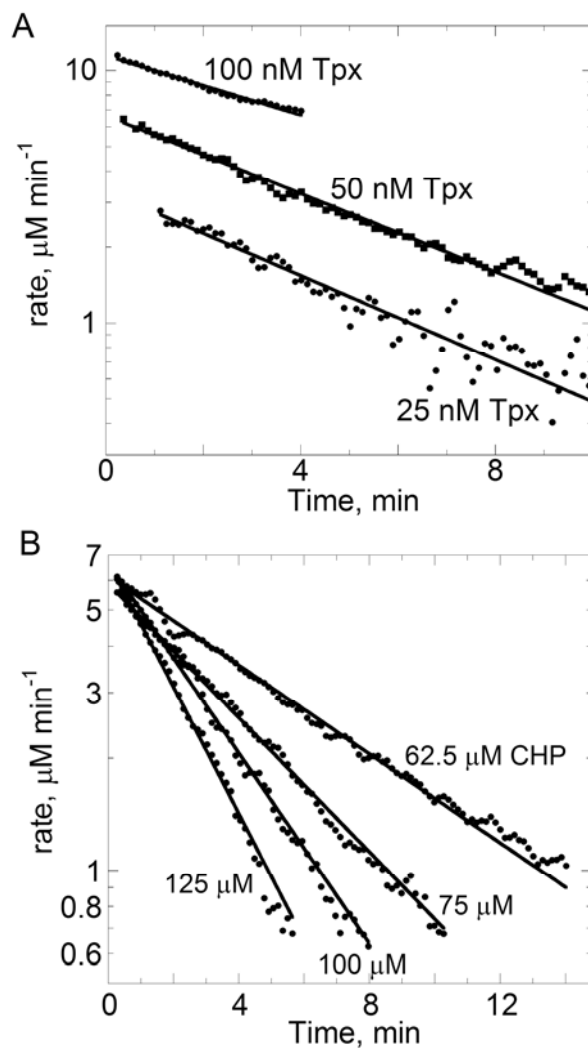


Fig. 4

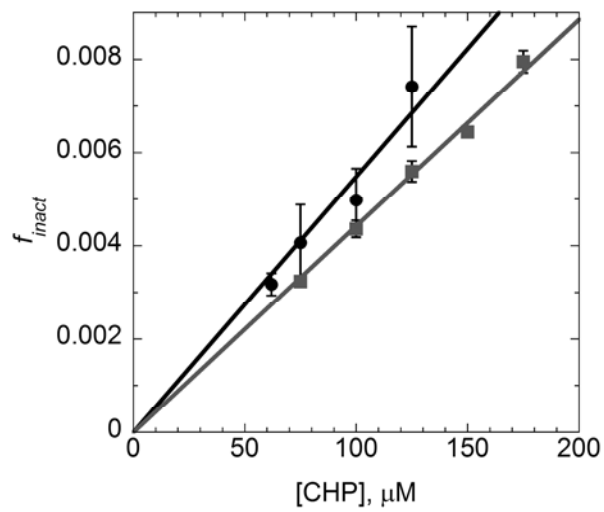


Fig. 5

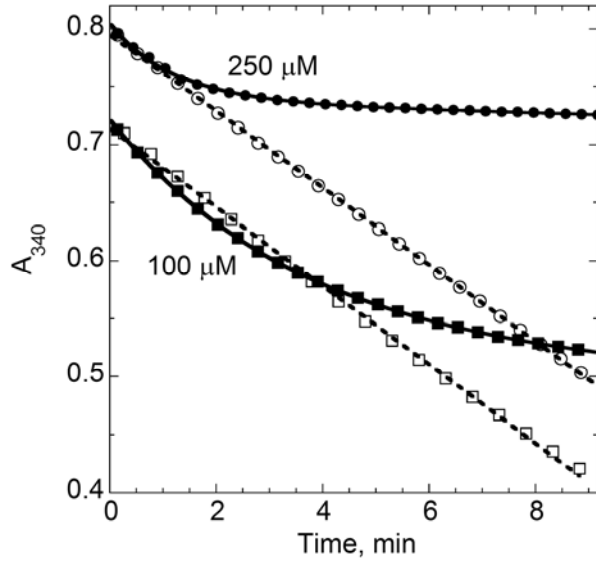


Fig. 6

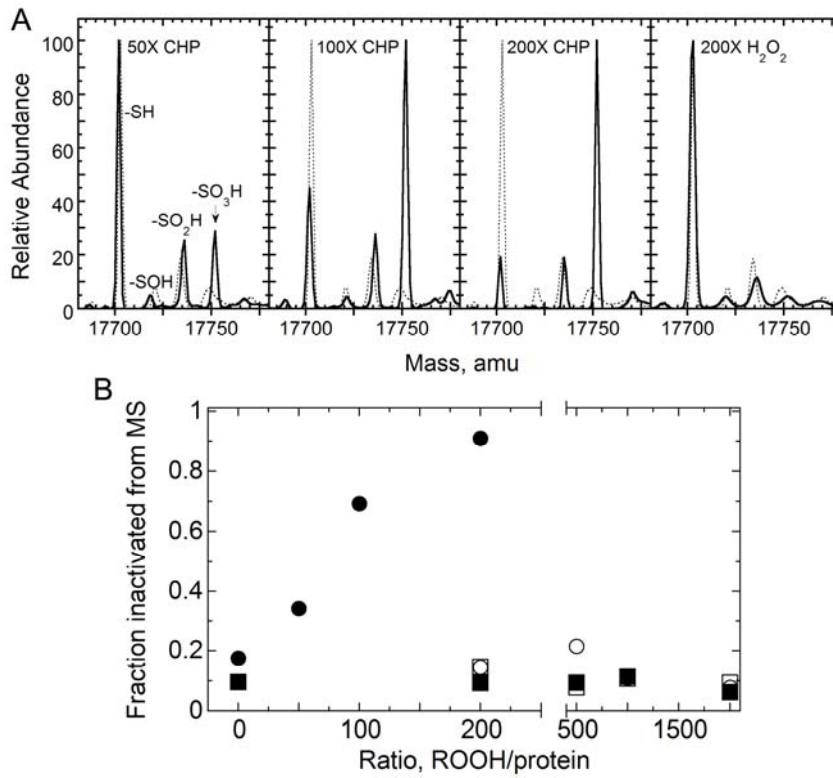


Fig. 7

